ELSEVIER

Surface and Coatings Technology 141 (2001) 141–144

SURFACE & COATINGS TECHNOLOGY

www.elsevier.nl/locate/surfcoat

Fe-based thick amorphous-alloy coating by laser cladding

Xiaolei Wu*,[1], Youshi Hong

State Key Lab of Nonlinear Mechanics, Institute of Mechanics, Chinese Academy of Sciences, Beijing 100080, PR China

Received 7 July 2000; accepted in revised form 3 April 2001

Abstract

New thick Fe-based amorphous alloy coatings have been synthesized by laser surface cladding, with the nominal composition of $Fe_{57}Co_8Ni_8Zr_{10}Si_4B_{13}$ (at.%). The supercooled liquid region, ΔT_x, defined by the difference between the glass transition temperature (T_g) and the onset temperature of crystallization (T_x) was as large as 62 K and T_g was 821 K. The high thermal stability of the supercooled liquid enabled the synthesis of a coating with maximum thickness of 1.2 mm. The amorphous alloy coating had a high Vickers hardness of 1270 and good corrosion resistance.

Keywords: Amorphous alloy; Laser cladding; Glass-forming ability; Coating

1. Introduction

There has been substantial and long-standing interest in producing amorphous alloy (*a*-alloy) layers on bulk crystalline substrates, in view of the attractive mechanical, physical and chemical properties of *a*-alloys [1–3]. High-energy laser treatment is one of surface amorphization techniques for synthesis of *a*-alloy layers in terms of: (i) a sufficiently fast cooling rate to avoid crystallization, (ii) a high solidification velocity such that solute trapping will occur and processes requiring large segregation no longer operate [4]. However, because of the necessity of high cooling rates above 10^5 K/s for the *a*-alloy formation, the resulting layer thickness was usually limited to less than 50 μm. From the early 1990s, a series of new bulk *a*-alloys with the multicomponent chemistry and excellent glass-forming ability (GFA) have been discovered in Zr-, Mg-, La-, Pd-, Ti-, and Fe-based systems [5–12] by various solidification methods. These bulk *a*-alloys revealed strong resistance to crystallization in the supercooled liquid state and excellent mechanical and physical properties. As far as Fe-based bulk *a*-alloys were concerned, Inoue et al. [13–18] found that Fe-(Al,Ga)-metalloid, Fe-TM-(Al,Ga)-metalloid (TM = Nb, Cr, Mo), (Fe,Co)-(Zr,Hf,Nb)-B and (Fe,Co)-(Zr,Hf,Ta)-(Mo,W)-B bulk *a*-alloys had thicknesses ranging up to approximately 2–6 mm and exhibited a large supercooled liquid region (~66–88 K). The large GFA of the Fe-based *a*-alloys was considered to be due to the satisfaction of three empirical rules [8]. The discovery of bulk *a*-alloys opened up bright prospects for the synthesis of thick *a*-alloy coatings with large GFA. The authors have carried out an exploratory study on the multicomponent Fe-based alloy coating by laser cladding. The process consisted of melting the substrate surface with pre-placed Fe-based alloy particles, allowing them to solidify rapidly, and then forming a surface coating with a structure, chemical composition and property different from those of the substrate. This paper presents the results on the alloy composition, thermal stability, hardness, and corrosion resistance of a thick *a*-alloy coating and discusses the reason for the large GFA. The novel *a*-alloy coating is believed to have considerable potential for advanced engineering materials due to their advantageous properties and

* Corresponding author. [1] Present address: Chemical Engineering Department, Cleveland State University, 1960 E24th St. SH 455, Cleveland, OH 44115, USA. Tel.: +1-216-523-7280; fax: +1-216-687-9220.

E-mail address: wuxl_cas@hotmail.com (X. Wu).

0257-8972/01/$ - see front matter
PII: S0257-8972(01)01263-4

excellent processing capabilities. To our knowledge, this was the first time that the synthesis of a thick *a*-alloy coating with the large GFA has been achieved by laser cladding.

2. Experimental procedure

Rectangular specimens of AISI 1045, 40 mm long, 30 mm wide and 20 mm thick were used as the substrate. A powder mixture was selected for laser cladding, with the nominal atomic percentage composition $Fe_{57}Co_8Ni_8Zr_{10}Si_4B_{13}$. The size and purity of particles were in the ranges from 6 to 44 μm and from 99.5 to 99.99 wt.%, respectively. The powders were evenly mixed in an argon gas atmosphere. The mixture paste was pre-coated onto the specimen surface using acetone, to a thickness of ~1.3 mm.

A 10-kW cw CO_2 laser was used to produce the coating. The laser was operated in a mode which resulted in an underfocused annulus-shaped incident beam having an outer diameter close to 3.5 mm and a Gaussian power distribution. This spatial distribution of the energy intensity is advantageous due to more uniform heating and low dilution effects. The processing parameters were a power of 7.5 kW and process speed of 50 mm/s. The specimen was in a shielding box where high-purity argon gas was continuously supplied to provide an inert environment with a positive gas pressure. Before laser processing, argon gas flowed through the box for 5 minutes.

The coating was characterized by Link-AN 1000 X-ray energy dispersive spectrometer (EDS) with a detecting error of less than 0.5%, Rigaku X-ray diffractometry (D/max-RB, 12 kW) with CoKα radiation, Neuphot-21 optical microscopy, and Philips EM 420 transmission electron microscopy (TEM). The thermal stability associated with glass transition, supercooled liquid, and crystallization was examined at a heating rate of 0.17 K/s by Perkin-Elmer differential scanning calorimeter (DSC) with a sensitivity of 0.02 mJ/s for energy. The melting temperature (T_m) was also measured by differential thermal analysis. All the specimens for X-ray diffraction (XRD), DSC and TEM analysis were thin slices. Thin slices of 100 μm thickness were taken using a slow-speed cut-off saw with a thickness of 100 μm, parallel to the top surface of the substrate. Successive cuts assured inspection at a well-identified depth of the whole coating. The final DSC specimen was 10 mm × 5 mm × 50 μm. Thin TEM films were mechanically thinned to 50 μm and then chemically polished in a solution of 35% nitric acid and 65% methanol in volume at 25°C below zero. The microhardness was measured at various depths across the thickness direction below the clad surface with a Vickers hardness tester under a 200 g load. Corrosion resistance was analyzed by weight loss after immersion in aqua regia for 3.6 ks at 297 K.

3. Results and discussion

Fig. 1a shows the low-magnification optical morphology of the cross-section of the coating, with a maximum thickness of approximately 1.2 mm. Fig. 1b is the high-magnification optical morphology at the bond region between the coating and the substrate. It is seen that the dendrites first grow epitaxially to a small degree at the interface between the substrate alloy and the coating and are then suppressed completely in the coating. The coating reveals a featureless contrast in an etched state using hydrogenfluoride acid or aqua regia.

Fig. 2 shows the distribution the alloy elements near the bond region between the coating and substrate. It is observed that the coating has a uniform distribution of alloy elements. The dilution of the alloy elements to a certain degree exists at the bond region between the coating and substrate.

Fig. 3 shows the X-ray diffraction pattern at a distance of 0.6 mm away from the top surface of the coating. Only a broad halo peak is seen and no diffraction peak corresponding to a crystalline phase is observed. Fig. 4 is bright-field (BF) TEM image and selected-area diffraction pattern (SADP) at a distance of approximately 0.6 mm away from the pool surface. BF reveals the absence of any crystalline phase and SADP also consists of halo rings typical of an *a*-alloy. Successive detection by XRD and TEM at various coating depths indicates the formation of the single *a*-alloy phase at a range from the pool depth of 0.8 mm to the pool top surface. Therefore, the *a*-alloy is formed in the pool. The epitaxial growth of the dendrites is suppressed at the interface between the coating and the substrate. That is, the cooling rate obtained by laser cladding is high enough to produce an *a*-alloy.

Fig. 5 shows the DSC curve of the *a*-alloy at a distance of 0.4 mm away from the top surface of the coating. The supercooled liquid region (SLR), ΔT_x,

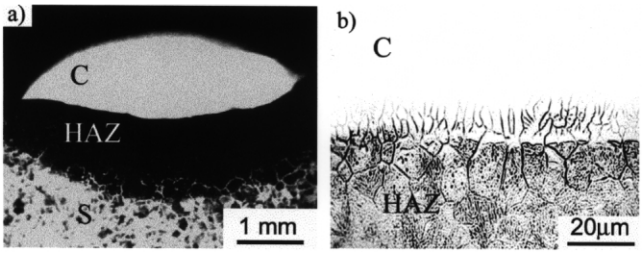

Fig. 1. Optical micrograph of the thick amorphous-alloy coating. (a) Low magnification cross-section (C, coating; HAZ, heat affected zone; S, substrate); (b) High magnification cross-section showing the bond region between the coating and substrate.

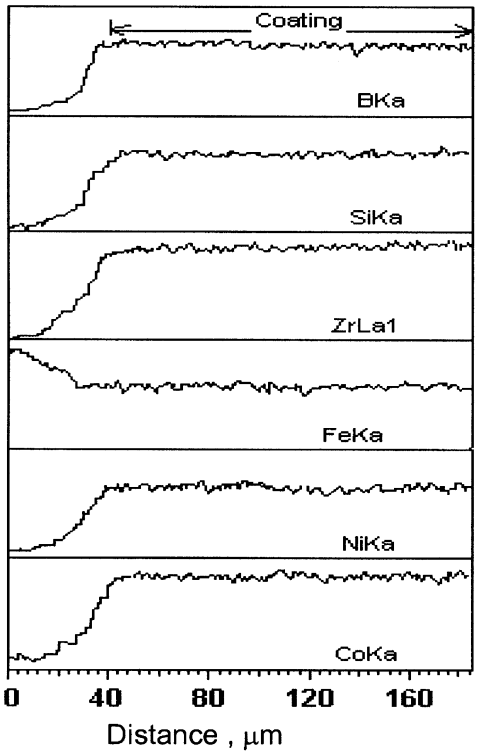

Fig. 2. Distribution of alloy elements in the clad coating by EDS.

defined by the difference between the glass transition temperature (T_g) and the onset temperature of crystallization (T_x) is as large as 62 K. The T_m measured is 1457 K for the present *a*-alloy and the reduced glass temperature, T_g/T_m was 0.61. Therefore, both ΔT_x and T_g/T_m values of the present *a*-alloy are in agreement with those of Fe-based bulk *a*-alloys by Inoue et al. [13–18].

The thick *a*-alloy coating has an average H_v as high as 1270. Besides, no weight loss is detected after immersion for 3.6 ks at 297 K in aqua regia. It is, therefore, concluded that the thick *a*-alloy coating possesses simultaneously large GFA, high hardness, and high corrosion resistance.

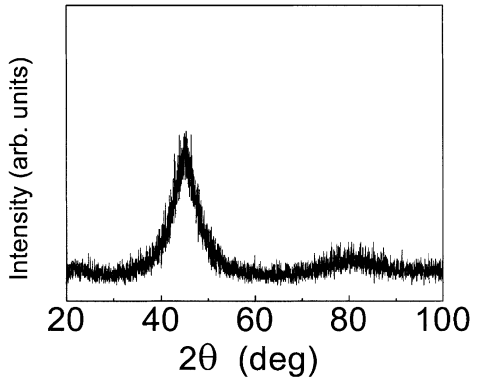

Fig. 3. X-Ray diffraction pattern of the coating at a distance of 0.6 mm away from the top surface of the coating.

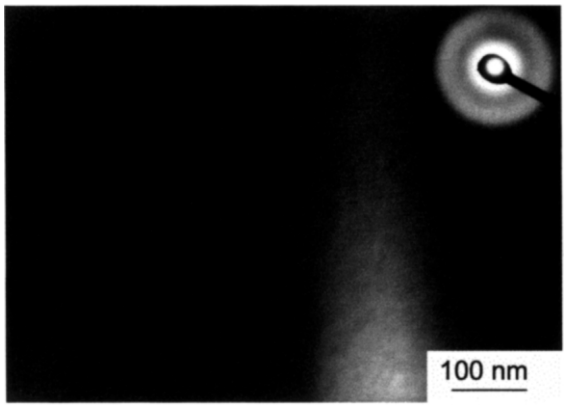

Fig. 4. Transmission electron bright-field micrograph showing the morphology of the amorphous alloy at a distance of 0.6 mm away from the top surface of the coating. Inset shows the halo ring diffraction pattern.

The present Fe-based thick *a*-alloy coating has a large GFA with high thermal stability. The mechanism for the large GFA can be interpreted in structural, thermodynamic, and kinetic aspects.

The GFA of the *a*-alloy is closely related to the atomic structure. Structurally, the base composition in the present *a*-alloy layer is the Fe–Zr–B system, which satisfies the three empirical rules proposed by Inoue et al. [8], i.e. (i) multicomponent alloy systems consisting of more than three constituent elements; (ii) significantly different atomic size ratios above approximately 13%; and (iii) suitable negative heats of mixing among the constituent elements. The effective addition of Co, Si and Ni causes the sequential change in the atomic size in the order of $Zr \gg Si > Fe > Ni > Co \gg B$, as well as the generation of new atomic pairs with various negative heats of mixing. The topological and chemical short-range order are enhanced, leading to the formation of highly dense random packed structure with low atomic diffusivity in the supercooled liquid [14]. The structural studies indicate that the highly dense, randomly packed structure of the novel *a*-alloy results

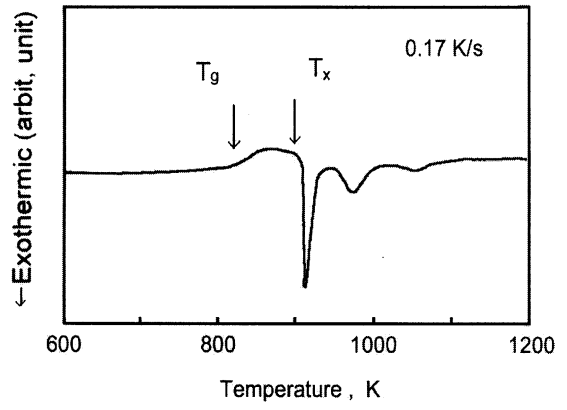

Fig. 5. DSC curve of the amorphous-alloy coating at a distance of 0.4 mm away from the top surface of the coating.

from large atomic size ratios in the multicomponent system [5,8,12]. This kind of structure suppresses nucleation and growth of the crystalline phase in the supercooled liquid state by inhibiting the long distance diffusion and increasing the melting viscosity. The structural features of the novel bulk *a*-alloy make the nucleation and growth of crystalline phases from the initially homogeneous supercooled liquid extremely difficult, because of the extremely slow mobility of the constituents in the high viscous supercooled liquid. It is very difficult for the six elements in the alloy to simultaneously satisfy the composition and structural requirements of the crystalline compounds. Therefore, the novel *a*-alloy has the large GFA.

The ΔT_x is 62 K and T_g/T_m is 0.61 for the present *a*-alloys. For the conventional Fe-B *a*-alloy, however, ΔT_x is only approximately $5 \sim 10$ K [19]. From the thermodynamic point of view, it is confirmed that the wide SLR has been generally found in good GFA *a*-alloys and the ΔT_x shows a good correlation with the GFA in the bulk *a*-alloy [8,11]. It is considered that large ΔT_x can be used to represent the GFA for the easy glass forming *a*-alloy. In addition, the larger the T_g/T_m ratio, the greater the GFA [5,8,12,16]. The multicomponent bulk *a*-alloy has a highly random close packing structure [20], and its composition and local structure are much different from those of the crystallization phase. The local atomic configuration of the short-range order and the composition in the conventional *a*-alloys resemble the corresponding equilibrium compounds with compositions near those of the *a*-alloys (for example, $MgZn_2$ Laves phase) [12]. The crystallization process occurs easily because it does not need long diffusion of atoms, so a high cooling rate is needed for suppressing nucleation and growth of the crystalline phase [12]. However, the highly random close packing structure and large viscosity make the redistribution of atoms on a large range scale extremely difficult. The greater the number of the components, the more difficult it is for all constituents to satisfy simultaneously the local structural and compositional requirements of crystalline phases. This argument is called 'the confusion principle' [21]. Kinetically, the large number of components and the structural features lead to an excellent GFA and high thermal stability [5,8,11].

4. Summary

A new and original Fe-based thick *a*-alloy coating with nominal composition $Fe_{57}Co_8Ni_8Zr_{10}Si_4B_{13}$ has been synthesized by laser surface cladding. The cooling rate obtained by laser cladding is high enough to produce an *a*-alloy in the coating. The maximum thickness of the coating is 1.2 mm. The supercooled liquid region, ΔT_x and the reduced amorphous-forming temperature, T_g/T_m are 62 K and 0.61, respectively. The *a*-alloy coating reveals high microhardness of 1270 and good corrosion resistance as well.

Acknowledgements

This research was supported by National Natural Science Foundation (Grant No.19891180), National Outstanding Youth Scientific Award of China (Grant No.19525205) and The Chinese Academy of Sciences.

References

[1] R.W. Cahn, Nature 260 (1976) 285.
[2] X.L. Wu, Y.S. Hong, Surf. Coating Technol. 132 (2000) 194.
[3] D.G. Morris, Mater. Sci. Eng. A 97 (1988) 177.
[4] F. Hirose, M. Takagi, H. Mori, Y. Kitoh, T. Imura, Jpn. J. Appl. Phys. 31 (1992) 3940.
[5] W.L. Johnson, Mater. Sci. Forum 225–227 (1996) 35.
[6] R. Busch, Y.J. Kim, W.L. John, J. Appl. Phys. 77 (1995) 4039.
[7] A. Peker, W.L. Johnson, Appl. Phys. Lett. 63 (1993) 2342.
[8] A. Inoue, Mater. Trans. JIM 36 (1995) 866.
[9] A. Inoue, T. Zhang, T. Masumoto, Mater. Trans. JIM 30 (1989) 965.
[10] A. Inoue, T. Zhang, T. Masumoto, J. Non-Cryst. Solids. 156–158 (1993) 473.
[11] W.H. Wang, Z.X. Bao, C.X. Liu, D.Q. Zhao, J. Eckert, Phys. Rev. B. 61 (2000) 3166.
[12] W.H. Wang, Q. Wei, S. Friedrich, M.P. Macht, N. Wanderka, H. Wollenberger, Appl. Phys. Lett. 71 (1997) 1053.
[13] A. Inoue, J.S. Gook, Mater. Trans. JIM 36 (1995) 1180.
[14] A. Inoue, Y. Shinohara, J.S. Gook, Mater. Trans. JIM 36 (1995) 1427.
[15] A. Inoue, J.S. Gook, Mater. Trans. JIM 37 (1996) 32.
[16] A. Inoue, T. Zhang, A. Takeuchi, Appl. Phys. Lett. 71 (1997) 464.
[17] A. Inoue, T. Zhang, T. Itoi, A. Takeuchi, Mater. Trans. JIM 38 (1997) 359.
[18] A. Inoue, H. Koshiba, T. Zhang, A. Makino, J. Appl. Phys. 83 (1998) 1967.
[19] H.A. Davies, in: F.E. Luborsky (Ed.), Amorphous Metallic Alloys, Butterworths, London, 1983, p. 8.
[20] R. Wang, Nature 278 (1979) 700.
[21] A.L. Greer, Nature 366 (1993) 303.